



Scholars Research Library

Der Pharma Chemica, 2010, 2(4): 342-360

(<http://derpharmachemica.com/archive.html>)



Vibrational spectra and assignment of 3-(2-Nitrophenoxy) phthalonitrile by Ab initio Hartree-Fock and Density Functional Methods

Neeraj Misra^{1*}, Anoop Pandey¹, Apoorva Dwivedi¹, Sanjeev Trivedi¹,
Shamoon Ahmad Siddiqui¹

¹Department of Physics, University of Lucknow 226007, India

ABSTRACT

This work deals with a theoretical study of the molecular structure of 3-(2-Nitrophenoxy) phthalonitrile. The equilibrium geometry, harmonic vibrational frequencies, infrared intensities in scattering activities was calculated by the ab initio Hartree-Fock method and the Density Functional B3LYP method employing 6-311g (d, p) as the basis set. A detailed interpretation of the infrared spectra of 3-(2-Nitrophenoxy) phthalonitrile is reported. The scaled theoretical wave numbers are in perfect agreement with the experimental values.

Keywords: FTIR Spectra, Molecular structure, 3-(2-Nitrophenoxy) phthalonitrile, Vibrational spectra.

INTRODUCTION

In recent years the synthesis of near infrared absorbing dyes has been an increasingly active field. Phthalonitriles (1,2-dicyanobenzenes) are used as synthetic precursors for large macrocyclic organic semiconductors, particularly for phthalocyanines [1,2] with strong absorption in the near infrared region of the spectrum. For the synthesis of substituted phthalocyanines, halogen substituted phthalonitriles are used. Vibrational studies of these precursor molecules are of interest in their own right and they are extremely valuable when performing vibrational studies of larger composite molecular systems. In the present work we are discussing on 3-(2-Nitrophenoxy) phthalonitrile. Several vibrational studies of different phthalonitriles have been carried out [3–7]. Phthalonitriles are among the most important precursors of phthalocyanine materials (Leznoff, 1989–1996). Monophenoxyphthalonitriles have

been used for preparing symmetrical phthalocyanines, which have been applied in many areas, such as laser printing, photocopying, optical data storage, and catalysis (McKeown, 1998) [8].

Computational Method

The entire DFT calculations were performed at Pentium IV (2.99GHz) personal computer using the Gaussian 98W, program package [9] utilizing gradient geometry optimization [10]. The vibrational frequencies associated with ground state optimized geometry have been evaluated with different level of theories and 6-311G (d, p) as the basis set. Use of HF and B3LYP with split valence basis set 6-311G (d, p) shows excellent compromise between accuracy and computational efficiency of vibrational spectra of large and medium molecules. It is well known that vibrational frequencies obtained by quantum chemistry calculations are typically larger than that of their experimental counterpart and thus experimental scaling factors are usually employed to have better agreement with the experimental vibrational frequencies [11]. These scaling factor depend on both basis set and method used in the calculation and are determined from the mean deviation between calculated and experimental value of frequencies [12,13]. On the other hand B exchange functional have advantage standard frequency very close to unity so B based procedures can be often used with out scaling [14-16]. The vibrational frequencies for given molecule were scaled [17] by .9630 and .8929 which is calculated with the B3LYP and HF methods respectively.

The Assignment of the calculated Normal Modes has been made on the basis of the corresponding to quantum chemically calculated vibrational frequencies using program. Gauss View 3.0 program [18] has been considered to get visual animation and also for the inspection of the Normal Modes Description.

RESULTS AND DISCUSSION

3.1 Molecular Geometry

The optimized structure parameters of 3-(2-Nitrophenoxy) phthalonitrile calculated by ab initio, HF and DFT, B3LYP levels with the 6-311G (d, p) basis set are listed in Table 1 in accordance given in Fig 1. The other calculated bond lengths also show an excellent agreement with experimental value. By allowing the relaxation of all parameters, the calculations converge to optimized geometries, which correspond to true energy minima, as revealed by the lack of imaginary frequencies in the vibrational mode calculation. Subsequently, the global minimum energy obtained for structure optimization of 3-(2-Nitrophenoxy) phthalonitrile with 6-311G(d,p) basis sets is approximately at -927A.U.&-922.for DFT/B3LYP and HF respectively . In case of 3-(2-Nitrophenoxy) phthalonitrile molecule the has no point group symmetry in calculation of all methods So 3-(2-Nitrophenoxy) phthalonitrile have C₁ molecular symmetry. Moreover, as described by the animated view of the output of 3-(2-Nitrophenoxy) phthalonitrile neither two oxygen in nitro group. Several bond lengths and bond angles of 3-(2-Nitrophenoxy) phthalonitrile are taken from the literature. The calculated bond lengths and bond angles are also in excellent agreement with experimental values. Thus, although there are some differences between the theoretical values and experimental values, the optimized structural parameters can well reproduce the experimental ones and they are the basis for the coming discussion. As it seems that the optimized bond lengths of C-C using B3LYP and HF method in ring R1 falls in the range from 1.390Å to 1.4301Å, and 1.382Å to 1.44Å respectively which are in good agreement with those of the experimental bond lengths [1.445Å-1.372Å]. The optimized bond

lengths of C-C in ring R2 falls in the range from 1.38Å to 1.394Å, and 1.379Å to 1.392Å which are also in good agreement with those of the experimental bond lengths [1.359Å-1.395Å]. The bond length between 10C-8C,9C-7C are 1.43Å,1.44Å in case experimental data however in case calculated data are corresponding calculated data are 1.43Å,1.44Å in case of HF method and 1.42Å,1.43Å in case of B3LYP method deviates substantially from usual bond length between C-C single bond 1.54. Dewar and Schmeising [19] attributed this to SP² hybridized state of C10,C9. The NBO analysis [20] shows that $\sigma_{C10-8C,C9-C7}$ NBO is formed from SP^{1.84}, hybrid on C10,C9 with SP^{2.23} hybrid on C8,C7. If the two rings are constrained to be coplanar weak intermolecular interaction in between 1O and 2O pushes two ring which causes H25 and 13H of phenyl ring too close to each other resulting in destabilization the Vander walls repulsion and hence both ring are attached to each other at an angle by 62.57⁰ with the oxygen atom. As described by the animated view of the output leads, no oxygen atom of nitro group lies in plane of corresponding benzene ring and also nitro group displaced with plane of corresponding ring.

Table: 1 Bond lengths & Bond Angle of 3-(2-Nitrophenoxy)phthalonitrile

Sl.No.	Parameters	Exp. Data	Theoretical Values	
		X-Ray Data	HF/6-311G(d,p)	B3LYP/6-311G(d,p)
1	O1-C11	1.377	1.3496	1.3654
2	O1-C18	1.398	1.3564	1.3782
3	O2=N6	1.214	1.1839	1.2223
4	O3=N6	1.213	1.1873	1.2214
5	N4≡C7	1.129	1.1292	1.1544
6	N5≡C8	1.136	1.1289	1.1545
7	N6-C19	1.452	1.4639	1.4762
8	C7-C9	1.445	1.4428	1.4301
9	C8-C10	1.443	1.4385	1.4262
10	C9-C10	1.403	1.394	1.4122

11	C9-C16	1.376	1.3849	1.3974
12	C10-C11	1.385	1.3906	1.4056
13	C11-C12	1.385	1.383	1.3921
14	C12-H13	0.930	1.0729	1.0814
15	C12-C14	1.372	1.3825	1.3904
16	C14-H15	0.930	1.0742	1.0832
17	C14-C16	1.383	1.3814	1.39
18	C16-H17	0.930	1.0726	1.0816
19	C18-C19	1.395	1.3923	1.399
20	C18-C24	1.372	1.3826	1.3922
21	C19-C20	1.390	1.3848	1.3921
22	C20-H21	0.930	1.0712	1.0816
23	C20-C22	1.359	1.3793	1.3886
24	C22-H23	0.930	1.0736	1.0828
25	C22-C26	1.372	1.3843	1.3943
26	C24-H25	0.930	1.0735	1.0831
27	C24-C26	1.369	1.382	1.3912
28	C26-H27	0.930	1.0746	1.0834

29	C11-O1-C18	119.6	122.6715	120.9743
30	O2=N6=O3	123.6	125.0389	125.4575
31	O2=N6-C19	119.0	118.0499	117.5099
32	O3=N6-C19	117.4	116.9085	117.0107
33	C7-C9-C10	118.7	120.6703	120.5094
34	C7-C9-C16	121.4	118.6351	119.213
35	C10-C9-C16	119.8	120.6945	120.2764
36	C8-C10-C9	120.5	121.3176	121.4253
37	C8-C10-C11	120.1	119.5712	119.7033
38	C9-C10-C11	119.3	119.1106	118.8698
39	O1-C11-C10	114.8	115.8186	115.4604
40	O1-C11-C12	124.5	123.7622	123.9567
41	C10-C11-C12	120.5	120.3801	120.5808
42	C11-C12-H13	120.3	120.2388	119.8089
43	C11-C12-C14	119.4	119.6473	119.6991
44	H13-C12-C14	120.3	120.1137	120.4863
45	C12-C14-H15	119.4	119.2994	119.3368
46	C12-C14-C16	121.1	120.9727	120.9716

47	H15-C14-C16	119.4	119.7274	119.6898
48	C9-C16-C14	119.8	119.1894	119.6017
49	C9-C16-H17	120.1	119.7751	119.409
50	C14-C16-H17	120.1	121.0352	120.9892
51	O1-C18-C19	117.4	124.5928	121.5335
52	O1-C18-C24	122.7	116.6207	119.0486
53	C19-C18-C24	119.9	118.7414	119.0577
54	N6-C19-C18	122.5	122.4517	121.549
55	N6-C19-C20	118.5	116.9578	117.6853
56	C18-C19-C20	119.0	120.5859	120.7645
57	C19-C20-H21	119.7	118.6157	118.463
58	C19-C20-C22	120.6	120.1738	119.7518
59	H21-C20-C22	119.7	121.2093	121.7851
60	C20-C22-H23	120.3	119.8494	119.7838
61	C20-C22-C26	119.5	119.4803	119.8063
62	H23-C22-C26	120.3	120.6696	120.4069
63	C18-C24-H25	120.2	117.9467	118.4758
64	C18-C24-C26	119.6	120.6386	120.2519

65	H25-C24-C26	120.2	121.4099	121.2555
66	C22-C26-C24	121.3	120.3724	120.3403
67	C22-C26-H27	119.3	120.1952	120.1553
68	C24-C26-H27	119.3	119.4322	119.4956

In the title compound (Fig. 1) the triple bond lengths between C and N, 1.136 (5) Å and 1.129 (5) Å, agree with Calculated value by both method but both bond length are not same to each other this is due to oxygen attached at ring extract more electron from the adjacent carbon this create efficiency at ortho position this effect reduce the bond strength of carbon and nitrogen so bond length between C-N increase. The geometry around the O atoms is in good agreement with the literature [21]. The calculated substituent impact on the C-C-C bond angles of the benzene ring is summarized in Table 2. The data reflects the well-known trends observed for various substituents: Groups with π -acceptor substituent tend to increase in α_{ipso} , decrease α_{ortho} and it results in a small increase in α_{para} . However, most of the substituents in the present study have a mixed σ/π character and the geometrical parameters of the ring are a result of superposition of overall effects.

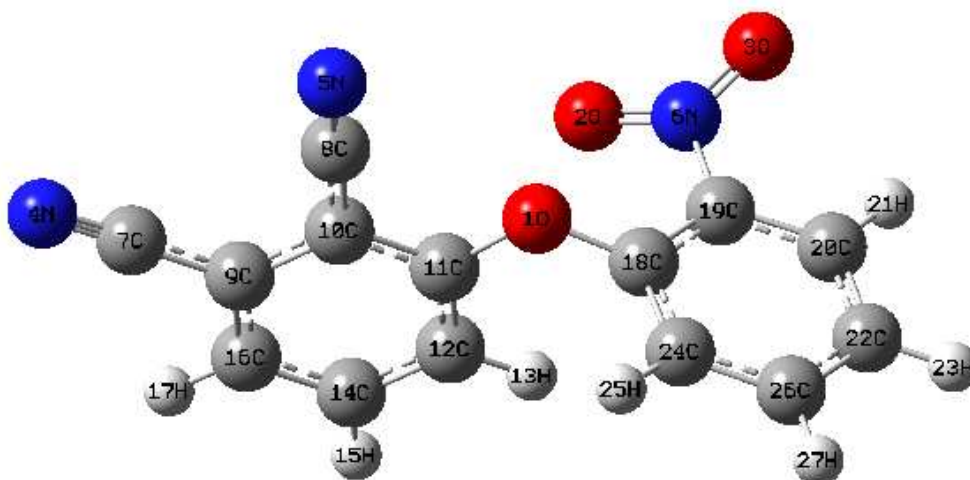


Figure-1 Model Molecular Structure of 3-(2-Nitrophenoxy) phthalonitrile

Table 2 Atomic Charge (e) of 3-(2-Nitrophenoxy) phthalonitrile in gas phase

SL.No.	Atom	HF/6-311G(d,p)	B3LYP/6-311G(d,p)
1	O ₁	-0.475538	-0.341925
2	O ₂	-0.353252	-0.254611
3	O ₃	-0.370225	-0.247744
4	N ₄	-0.297801	-0.193355
5	N ₅	-0.30216	-0.190504
6	N ₆	0.336895	0.165526
7	C ₇	0.101215	0.019792
8	C ₈	0.151336	0.076093
9	C ₉	0.068442	0.018693
10	C ₁₀	0.030847	0.010463
11	C ₁₁	0.29653	0.211755
12	C ₁₂	-0.100133	-0.059656
13	H ₁₃	0.13783	0.120251
14	C ₁₄	-0.053453	-0.082163
15	H ₁₅	0.124318	0.11846
16	C ₁₆	-0.042616	-0.017063
17	H ₁₇	0.122537	0.117965
18	C ₁₈	0.239656	0.106684
19	C ₁₉	0.109497	0.145921
20	C ₂₀	-0.01157	-0.028787
21	H ₂₁	0.159698	0.141325
22	C ₂₂	-0.103847	-0.087253
23	H ₂₃	0.120545	0.117631
24	C ₂₄	-0.098604	-0.043492
25	H ₂₅	0.129961	0.123648
26	C ₂₆	-0.043895	-0.067103
27	H ₂₇	0.123787	0.11945

Other Molecular Properties

Several calculated Thermodynamic properties Based on the vibrational analysis at HF and B3LYP/6-311G (d, p) level, statistical Thermodynamics, the standard Thermodynamic functions internal thermal energy (E), constant volume heat capacity C_v and entropy S have been calculated and listed in Table 3. At the room temperature conduction band is almost empty so electronic contribution in total energy is negligible. Thermodynamic parameters clearly indicate that vibration motion plays a crucial role in order to assess the Thermo dynamical behavior of title compounds. Based on the vibrational analysis at HF and B3LYP/6-311G (d, p) level and statistical Thermodynamics, the standard thermodynamic functions internal thermal energy (E), constant volume dipole moment, zero point energy calculated by HF method are at larger value than B3LYP method however entropy S and heat capacity gave reverse result.

**Table 3 Thermodynamic Properties of 3-(2-Nitrophenoxy)phthalonitrile
(with 6-311G(d,p) Basis Sets)**

	HF/6-311G(d,p)	B3LYP/6-311G(d,p)
Total Thermal Energy	133.991	125.666
Vibrational Energy	132.214	123.888
Entropy	129.073	132.925
Rotational Energy	0.889	0.889
C_v	56.491	60.718
Zero Point Energy	-922.21698825	-927.71117547
Dipole Moment	11.1227	10.3539

3.2 Atomic Charge Distributions In Gas Phase

The Mulliken atomic charges for all the atoms of the compounds are calculated by HF and B3LYP /6-311G (d, p) levels in gas phase are presented in Table 2. To clarify the nature of the both molecule NBO and Mulliken, analyses were carried out. The most probable active site of 3-(2-Nitrophenoxy) phthalonitrile and the receptor binding on to these sites are adjacent of ring R1&R2 at O1atoms and N5 in ring R1 are having more negative and positive charge respectively. Another aspect also observed is that the atomic charges calculated by HF method are typically larger in magnitude than calculated by B3LYP method.

3.3 Assignment of Fundamentals

The molecule has 27 atoms and 75 normal modes of fundamental vibration. Out of 75 normal modes N-1 modes corresponding to the stretching modes and reaming are bending modes so 26 are stretching and 51 are bending modes. Whole assignment modes are divided in to part one corresponding to below 1000 cm^{-1} called finger print region and other corresponding to the above 1000 cm^{-1} called functional group region. Detailed description of vibrational modes can be given by means of normal coordinate analysis. The assignments of the experimental wave numbers based on normal mode analyses and a comparison with the theoretically scaled ones are provided in the Table 4&5. However the scaled vibrational signatures using all other methods are

also presented. In these cases the assignments are done following the animated view of normal mode description. It is to be emphasized that the calculated frequencies represent vibrational signatures of the molecules in its gas phase. Hence, the experimentally observed spectra of the solid/liquid samples may differ to some extent from the calculated spectrum. Moreover, the calculated harmonic force constants and frequencies are usually higher than the corresponding experimental quantities, due to combination of electron correlation of data, the calculated Raman data are illustrated only for B3LYP& HF 6-311G(d,p) method effects and basis set deficiencies. This is the reason to use scaling factor for theoretical calculations. Nevertheless, after applying the uniform scaling factor the theoretical calculation reproduce the experimental data well. The observed slight disagreement between the theory and the experiment could be a consequence of the anharmonicity and of the general tendency of the quantum chemical methods to overestimate the force constants at the exact equilibrium geometry. On the basis of our calculations and the reported FTIR Spectra (Fig 2)[22], we made a reliable one-to-one correspondence between our fundamentals and the frequencies calculated by HF and DFT methods. The detailed vibrational assignments are achieved by comparing the band positions and intensities observed in FT-IR with wave numbers and intensities from molecular modeling calculations at HF/6-311G (d, p) and B3LYP/6-311G (d, p) level and are given in Table 4 & 5.

TABLE 4

COMPARISON OF THE OBSERVED AND CALCULATED VIBRATIONAL SPECTRA OF 3-(2-NITROPHENOXY)PHTHALONITRILE (WITH HF/6-311G(D,P) BASIS SET)

S.No	HF/6-311G(d,p) Scaled freq.	FT IR IR Intensit y	Assignment Exp.
1	18	0.09	(O-Ring B Twist)
2	22	3.23	(O-Ring B Twist)
3	40	0.77	(C-NO ₂) Rock
4	65	0.98	□(C-O-C) adj ring A+Twist(C-NO ₂) Ring B
5	82	1.89	□(C-C-C) Ring A
6	119	2.58	□N-C-C) Ring A+Ring Twist About IO Ring B
7	126	3.94	□C-C-C) Ring B+□(N-C-C) Ring A
8	144	0.67	□(N-C-C) Ring A+□(C-NO ₂) Ring B
9	166	3.31	□(C-C-C) Ring A+□(N-C-C)Ring A
10	200	3.00	□(C-C-C) Ring A+□(N-C-C) Ring A

11	247	0.98		$\square(\text{C-O-C})\text{Ring Link} + \square(\text{C-C-C})\text{ Ring B} + \square(\text{N-C-C})\text{ Ring A}$
12	264	4.07		$\square(\text{O-N-O})\text{ Ring B} + \square(\text{C-O-C})\text{ Ring Link}$
13	278	2.95		$\square(\text{N-C-C})\text{ Ring A} + \square(\text{O-C-C})\text{ Ring Link}$
14	358	0.69		$\square(\text{N-C})\text{ Ring A} + \square(\text{C-C-C})\text{ Ring A} + \square(\text{C-O-C})\text{ Ring Link}$
15	376	0.01		$\square(\text{C-C-C})\text{ Ring A} + \square(\text{N-C-C})\text{ Ring A}$
16	395	1.86		$\square(\text{H-C})\text{Ring B} + \square(\text{C-C-C})\text{ Ring B}$
17	401	1.98		$\square(\text{C-C-C})\text{ Ring A}$
18	435	3.54	460	$\square(\text{H-C})\text{Ring A} + \square(\text{C-C-C})\text{ Ring B}$
19	445	0.30		$\square(\text{C-C-C})\text{ Ring A} + \square(\text{C-C-C})\text{ Ring A}$
20	464	6.34		$\square(\text{H-C})\text{ Ring A} + \square(\text{N-C-C})\text{ Ring A}$
21	502	9.31	520	$\square(\text{C-H})\text{ Ring B} + \square(\text{N-C-C})\text{ Ring A}$
22	549	2.12		$\square(\text{H-C})\text{ Ring B} + \square(\text{C-C-C}) + \square(\text{N-C-C})\text{ Ring B}$
23	554	2.42		$\square(\text{H-C})\text{ Ring B} + \square(\text{N-C-C})\text{ Ring A}$
24	562	2.17		$\square(\text{H-C})\text{ Ring A} + \square(\text{N-C-C})\text{ Ring A}$
25	573	1.61	590	$\square(\text{C-C-C})\text{ Ring B} + \square(\text{C-C-C})\text{ Ring A}$
26	618	4.21	639	$\square(\text{C-C-C})\text{ Ring A} + \square(\text{N-C-C})\text{ Ring A}$
27	625	1.22		$\square(\text{N-C-C-C})\text{ Ring A} + \square(\text{C-C-C})\text{ Ring B}$
28	646	11.52		$\square(\text{H-C})\text{ Ring B} + \square(\text{N-C-C-C})\text{ Ring A}$
29	658	3.87		Ring Deformation
30	712	26.42	721	$\square(\text{H-C})\text{ Ring B} + \square(11\text{C-1O-18C}) + \square(\text{C-NO}_2)\text{ Ring B}$
31	744	11.54		$\square(\text{H-C})\text{ Ring A}$
32	756	12.76		$\square(\text{H-C})\text{ Ring B} + \square(11\text{C-1O-18C}) + \square(\text{C-NO}_2)\text{ Ring B}$
33	770	44.96		$\square(\text{H-C})\text{ Ring B} + \square(\text{C-C-C})\text{ Ring A} + \square(\text{C-NO}_2)\text{ Ring B}$
34	796	4.47		$\square(\text{H-C})\text{ Ring B} + \square(\text{C-C-C})\text{ Ring A}$
35	799	19.95		$\square(\text{H-C})\text{ Ring A}$
36	813	48.19	814	$\square(11\text{C-1O-18C}) + \square(2\text{O-6N-3O}) + \square(\text{H-C})\text{ Ring B}$
37	869	28.41		$\square(2\text{O-6N-3O}) + \square(\text{C-C-C})\text{ Ring B}$
38	892	4.18		$\square(\text{C-H})\text{ Ring B}$
39	911	30.01	877	Ring out of plane bending in Ring B

40	957	70.70	935	\square (C-C-C) Ring A + \square (CH) Ring A
41	982	3.58		\square (C-H) Ring A
42	994	0.59	938	\square (8C-10C-11C-12C)
43	1003	0.45	970	\square (H-C-C-H) Ring B
44	1012	4.19		Ring B Breathing
45	1043	60.59	1055	Ring A Breathing
46	1062	48.66	1060	\square (C-C) Ring B + \square (CH) Ring A, B
47	1076	19.77	1110	\square (C-H) Ring B + \square (C-C) Ring A
48	1080	97.35		\square (C-C-C) Ring B + \square (CH) Ring B
49	1129	5.68	1150	\square (C-C-C) Ring B + \square (C-NO ₂) Ring B
50	1154	2.33	1200	\square (C-C-C) Ring A + \square (C-CN) Ring B
51	1169	3.65		\square (CH) Ring A
52	1176	43.53	1225	\square (CH) Ring B
53	1207	9.04		\square (C-C-C) Ring A, B + \square (CH) Ring A, B
54	1224	8.88		\square (C-H) Ring A, B
55	1245	47.67		\square (C-H) Ring A, B
56	1280	22.34	1270	\square (C-C) Ring B + \square (C-H) Ring B
57	1428	380.14	1375	\square (C-C) Ring B + \square (C-H) Ring B
58	1443	145.87		\square (C-C) Ring A + \square (C-H) Ring A
59	1450	15.34		\square (C-C-C) Ring A + \square (CH) Ring A
60	1460	347.96		\square (C-C) Ring A, B + s(NO ₂) Ring B
61	1470	82.44	1490	\square (C-C) Ring B + \square (C-H) Ring B
62	1572	42.23		\square (C-C) Ring A, B + \square (CH) Ring A, B
63	1577	151.68	1530	\square (C-C) Ring A, B + \square (CH) Ring A, B
64	1591	20.36		\square (C-C) Ring A, B + (CH)A, B
65	1595	63.85	1610	\square (C-C) Ring A, B + (CH)A, B
66	1653	620.09	1850	\square (C-C) Ring B + \square_{assym} (NO ₂) Ring B
67	2322	12.48	2225	\square (C-N) + \square (7C-4N) Ring A
68	2323	21.81		\square (C-N) Ring R1 both + (C-N)

69	2984	3.32		□(C-H) Ring B
70	2989	4.05		□(C-H) Ring A
71	3000	9.09		□(C-H) Ring B
72	3007	2.47		□(C-H) Ring B
73	3008	2.23		□(16C-17H)+ □(12C-13H)
74	3014	1.42		□(C-H) Ring A
75	3033	40.63	3100	□(20C-21H)+ □(22C-23H)

Abbreviations:

w-weak; vs.-very strong; s-strong; m-middle; sh-shoulder; v: stretching; ν_s : symmetric stretching ν_{as} : asymmetric stretching, β : -in plane bending; γ : out of plane bending, τ : torsion, F.C.: force constant.

TABLE- 5

COMPARISON OF THE OBSERVED AND CALCULATED VIBRATIONAL SPECTRA OF 3-(2-NITROPHENOXY)PHthalONITRILE (WITH B3LYP/6-311G(D,P) BASIS SET)

S. No	B3LYP/6-311G(d,p)		FT IR		Assignment
	Scaled freq.	IR Intensity	IR Intensity	Exp.	
1	18	1.46			(O-Ring B Twist)
2	30	2.80			(O-Ring B Twist)
3	51	0.30			(C-NO ₂) Rock
4	74	1.22			□(C-O-C) adj ring A+Twist(C-NO ₂) Ring B
5	75	1.55			□(C-C-C) Ring A
6	114	1.88			□N-C-C) Ring A+Ring Twist About 1O Ring B
7	121	2.67			□C-C-C) Ring B+□(N-C-C) Ring A
8	141	0.41			□(N-C-C) Ring A+□(C-NO ₂) Ring B
9	163	2.36			□(C-C-C) Ring A+□(N-C-C)Ring A
10	191	2.74			□(C-C-C) Ring A+□(N-C-C) Ring A
11	231	0.80			□(C-O-C)Ring Link+□(C-C-C) Ring B+□(N-C-C) Ring Δ

12	240	0.41		\square (O-N-O) Ring B+ \square (C-O-C) Ring Link
13	290	1.92		\square N-C-C) Ring A+ \square O-C-C) Ring Link
14	342	1.95		\square $\tilde{\square}$ N-C) Ring A+ \square \square -C-C) Ring A+ \square (C-O-C) Ring Link
15	369	0.02		\square C-C-C) Ring A+ \square (N-C-C) Ring A
16	397	1.20		\square (H-C)Ring B+ \square C-C-C) Ring B
17	400	0.73		\square C-C-C) Ring A
18	433	4.55	460	\square (H-C)Ring A+ \square (C-C-C) Ring B
19	447	0.71		\square C-C-C) Ring A+ \square \square -C-C) Ring A
20	454	5.31		\square (H-C) Ring A+ \square (N-C-C) Ring A
21	495	7.18	520	\square (C-H) Ring B+ \square (N-C-C) Ring A
22	548	0.62		\square (H-C) Ring B+ \square (C-C-C)+ \square (N-C-C) Ring B
23	554	1.42		\square (H-C) Ring B+ \square (N-C-C) Ring A
24	557	1.35		\square (H-C) Ring A+ \square (N-C-C) Ring A
25	573	0.68	590	\square C-C-C) Ring B+ \square \square -C-C) Ring A
26	608	4.57	639	\square (C-C-C) Ring A+ \square (N-C-C) Ring A
27	624	0.67		\square (N-C-C-C) Ring A+ \square (C-C-C) Ring B
28	648	2.64		\square (H-C) Ring B+ \square (N-C-C-C) Ring A
29	654	5.57		Ring Deformation
30	692	42.13	721	\square (H-C) Ring B+ \square (11C-1O-18C) + \square (C-NO ₂) Ring B
31	730	18.74		\square (H-C) Ring A
32	755	20.91		\square (H-C) Ring B+ \square (11C-1O-18C) + \square (C-NO ₂) Ring B
33	767	10.64		\square (H-C) Ring B+ \square (C-C-C) Ring A+ \square C-NO ₂) Ring B
34	770	17.17		\square (H-C) Ring B+ \square (C-C-C) Ring A
35	783	35.06		\square H-C) Ring A
36	801	67.16	814	\square (11C-1O-18C)+s(2O-6N-3O)+ \square (H-C) Ring B
37	843	30.92		s(2O-6N-3O)+ \square (C-C-C) Ring B
38	863	0.92		\square (C-H) Ring B
39	877	40.32	877	Ring out of plane bending in Ring B
40	942	2.44	935	\square (C-H) Ring B

41	955	0.17		\square (C-C-C) Ring A + \square (CH) Ring A
42	966	61.44	938	\square (8C-10C-11C-12C)
43	969	0.52	970	\square (H-C-C-H) Ring B
44	1020	3.38		Ring B Breathing
45	1056	62.93	1055	Ring A Breathing
46	1066	44.77	1060	\square (C-C) Ring B + \square (CH) Ring A, B
47	1121	8.93	1110	\square (C-H) Ring B + \square (C-C) Ring A
48	1142	5.23		\square (C-C-C) Ring B + \square (CH) Ring B
49	1154	2.12	1150	\square (C-C-C) Ring B + \square (C-NO ₂) Ring B
50	1169	2.66	1200	\square (C-C-C) Ring A + \square (C-CN) Ring B
51	1196	53.53		\square (CH) Ring A
52	1216	2.60	1225	\square (CH) Ring B
53	1239	23.16		\square (C-C-C) Ring A, B + \square (CH) Ring A, B
54	1250	407.70		\square (C-H) Ring A, B
55	1277	31.30		\square (C-H) Ring A, B
56	1291	41.46	1270	\square (C-C) Ring B + \square (C-H) Ring B
57	1336	234.86	1375	\square (C-C) Ring B + \square (C-H) Ring B
58	1424	4.20		\square (C-C) Ring A + \square (C-H) Ring A
59	1427	144.33		\square (C-C-C) Ring A + \square (CH) Ring A
60	1439	54.18		\square (C-C) Ring A, B + s(NO ₂) Ring B
61	1455	65.90	1490	\square (C-C) Ring B + \square (C-H) Ring B
62	1546	35.45		\square (C-C) Ring A, B + \square (CH) Ring A, B
63	1550	288.44	1530	\square (C-C) Ring A, B + \square (CH) Ring A, B
64	1566	29.64		\square (C-C) Ring A, B + (CH) A, B
65	1570	26.23	1610	\square (C-C) Ring A, B + (CH) A, B
66	1591	146.20	1850	\square (C-C) Ring B + \square _{assym} (NO ₂) Ring B
67	2257	12.36	2225	\square (C-N) + \square (7C-4N) Ring A
68	2260	3.60		\square (C-N) Ring R1 both + (C-N)
69	3065	1.91		\square (C-H) Ring B

70	3071	3.43		□(C-H) Ring A
71	3078	6.29		□(C-H) Ring B
72	3085	2.03		□(C-H) Ring B
73	3091	1.42		□(16C-17H)+ □(12C-13H)
74	3096	1.16		□(C-H) Ring A
75	3099	32.03	3100	□(20C-21H)+ □(22C-23H)

Abbreviations:

w-weak; vs.-very strong; s-strong; m-middle; sh-shoulder; v: stretching; ν_s : symmetric stretching ν_{as} : asymmetric stretching, β : -in plane bending; γ : out of plane bending, τ : torsion, F.C.: force constant.

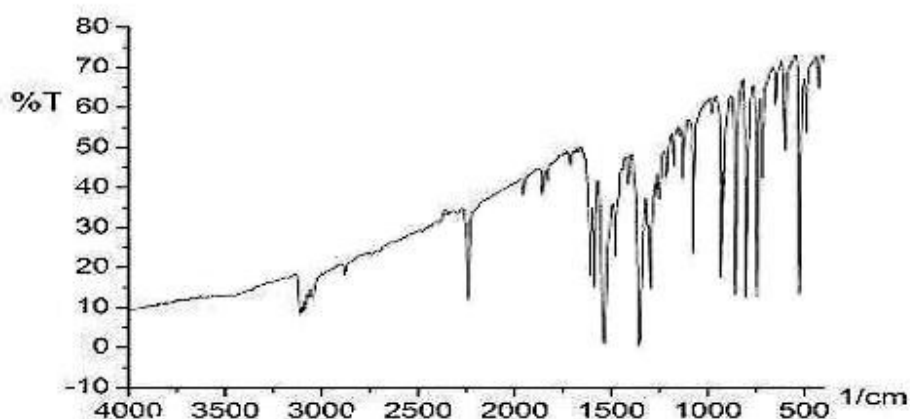


Figure-2 : FTIR Spectra of 3-(2-Nitrophenoxy) phthalonitrile

3.4 Vibrational Modes Description

3.4.1 C-H vibrations

The hetero aromatic structure shows the presence of C-H stretching vibrations in the region 3000-3100 cm^{-1} , which is the characteristic region for the ready identification of the C-H stretching vibration [23]. In this region bands are not affected appreciably by nature of substituent. In the present study the C-H stretching vibration of the title compound is observed at 3100 cm^{-1} , which is in good agreement with the calculated frequency at 3033 cm^{-1} for HF and at 3099 cm^{-1} for B3LYP method. In the range from 3099-3065 cm^{-1} and 3033-2984 cm^{-1} some other C-H stretching vibrations are also calculated by B3LYP, HF method respectively which are supported by the observed ones. No peaks of these modes are more significant intensity in case of IR spectra. A medium intense band are calculated at 813 cm^{-1} , for HF 801 cm^{-1} , for B3LYP method respectively which is due to mixing of several band along with C-H out of plane bending in ring B are supported by literature and observed FTIR value obtained at 814 cm^{-1} . Some

bending vibrations of C-H are also calculated and supported by literature. At lower frequencies region some significant intensity peaks of polarized IR due to out of plane bending in C-H are occurred.

3.4.2 C-C Vibrations

With heavy substituent, the band tend to shift some what lower wavenumber and greater the number of substituent on the ring broader the absorption region [24]. The C-C aromatic stretch known as semi-circle stretching, calculated at 1591-1066 cm^{-1} for B3LYP method and 1653-1062 cm^{-1} for HF method respectively, may be describe as opposite quadrant of ring stretching while intervening quadrants contract and is supported by literature [25] Two conjugative intense modes which is due to mixing of several modes along with the C-C aromatic stretch known as semi-circle stretching, calculated at 1653 & 1595 cm^{-1} for HF and at 1591 & 1570 cm^{-1} for B3LYP method respectively, are in perfect agreement with the observed frequencies at 1610 & 1575 cm^{-1} . At lower sides of calculated modes are due to in plane and out of plane bending of the ring of insignificant intensity. Vibration is describe that every carbon of sextant going up out of the plane while intervening carbon of sextant going down of plane are also supported by experimental data.

3.4.3 C-CN and C-NO₂ Vibrations

In this study the C-CN stretching vibration is calculated at 1169 cm^{-1} , and 1154 cm^{-1} for using B3LYP, HF respectively which is in good agreement with the observed frequency obtained 1200 cm^{-1} . Some other mixing of different modes of vibration along with C-NO₂ stretching are also occurred at lower side of calculated data at 1154 cm^{-1} and 1129 cm^{-1} of B3LYP and HF method respectively well matched with experimental data at 1150 cm^{-1} . Any deviation in C-NO₂ between experimental and calculated wavenumber for this mode can be attributed to underestimation of large degree of π -electron delocalization due to conjugation or formation of hydrogen bonds.[26] The increase in conjugation generally lead to intensification of IR lines and band intensity. The conjugation and influence of intermolecular hydrogen bonding result in lowering of stretching frequency.

3.4.4 C \equiv N Vibrations

The identification of C \equiv N vibrations is a difficult task, since the mixing of vibrations is possible in this region. In this study a medium intense peak observed corresponds to the C \equiv N stretching vibrations are calculated at 2323 cm^{-1} for HF and at 2257 cm^{-1} for B3LYP method respectively and these are supported by observed frequency at 2225. It is difficult to identify that contribution of which is stretching is more due to their identical situation. But as it can see that HF method overestimated this band of frequency by 98 cm^{-1} however B3LYP method nearly superimposes to experimental ones. Several authors have performed extensive work developing empirical relationships between the equilibrium bond length and force constant [27,28]. These empirical relations demonstrate what one thinks of intuitively: those shorter stronger bonds have higher vibrational frequencies. The electron transfer into and localized in the CN antibonding orbital results in the significant reduction of cyano bond order and this leads to the appearance of CN stretching frequency at 2323 cm^{-1} (HF). Molecular orbital calculations at HF level and B3LYP level using 6-311G(d,p) basis set supports this interpretation. As expected the ring torsion modes appear in the observed low frequency range.

CONCLUSIONS

All frequencies are real in the molecule. Hence, compounds have stable structure. All calculations are done on a molecule so we ignore inter-molecular forces i.e. Vander-walls, molecule-molecule interaction. These interactions produce perturbation in energy levels resulting in increase or decrease of energy levels. As seen in Table 3, thermal energy calculated by B3LYP methods gave higher value while HF gave lowest value however, in the case of entropy vice versa is obtained. Considering the fact that the observed frequencies in solid and molten states involve anharmonicity [29], the comparison is made with the theoretical study in gas phase of the molecules. Among methods, B3LYP hybrid functional, applied to density functional force fields with a 6-311G (d, p) basis set most successfully reproduces the vibrational spectra of 3-(2-Nitrophenoxy) phthalonitrile. Theoretical mode description makes easy to identify the relatively weak IR more accurately. Furthermore, yet again it is established obviously that the scaled quantum mechanical method in combination with DFT may be used as a reliable tool for the interpretation of vibrational signatures. Some deviation occurred between experimental value and calculated result due to the incomplete approximation of basis set, electron-electron correlation [30] and anharmonicity which are not calculated in the present in calculated data. Some intensity are not well matched with experimental data this is due to the impurity of sample taken in experiment mixing of different modes so it is difficult to identify these modes and also intensity increases with intermolecular interaction in case of experimental data.

Acknowledgements

One of the authors (NM) is grateful to UGC, New Delhi for providing the financial assistance.

REFERENCES

- [1] P.J. Brach, S.J. Grammatica, O.A. Ossanna, L. Weinberger, *J. Heterocyc. Chem.* 7 (1970) 1403.
- [2] J.A. Elvidge, R.P. Linstead, *J. Chem. Soc.* 3536, (1995)
- [3] M.C. Castro-Pedrozo, G.W. King, *J. Mol. Spectrosc.* 73, (1978), 386.
- [4] C.G. Barraclough, H. Bissett, P. Pitman, P.J. Thistlethwaite, *Aust. J. Chem.* 30 (1977) 753.
- [5] J.F. Arenas, J.I. Marcos, F.J. Ramirez, *Spectrochim. Acta* 44A, (10), (1988), 1045.
- [6] J.F. Arenas, J.I. Marcos, F.J. Ramirez, *Can. J. Spectrosc.* 34 (1), (1989), 7.
- [7] J.T. Lopez Navarrete, J.J. Quirante, M.A.G. Aranda, V. Hernandez, F.J. Ramirez, *J. Phys. Chem.* 97, (1993), 10561.
- [8] Xian-Fu Zhang, Dandan Jia, Aijun Song and Qiang Liu, *Acta Cryst.* (2008), E64, o356.
- [9] M.J. Frisch, G.W. Trucks, H.B. Schlegel, G.E. Scuseria, M.A. Robb, J.R. Cheeseman, J.A. Montgomery Jr., T. Vreven, K.N. Kudin, J.C. Burant, J.M. Millam, S.S. Iyengar, J. Tomasi, V. Barone, B. Mennucci, M. Cossi, G. Scalmani, N. Rega, G.A. Petersson, H. Nakatsuji, M. Hada, M. Ehara, K. Toyota, R. Fukuda, J. Hasegawa, M. Ishida, T. Nakajima, Y. Honda, R. O. Kitao, H. Nakai, M. Klene, X. Li, J.E. Knox, H.P. Hratchian, J.B. Cross, C. Adamo, J. Jaramillo, Gomperts, R.E. Stratmann, O. Yazyev, A.J. Austin, R. Cammi, C. Pomelli, J.W. Ochterski, P.Y. Ayala, K. Morokuma, G.A. Voth, P. Salvador, J.J. Dannenberg, V.G. Zakrzewski, S. Dapprich, A.D. Daniels, M.C. Strain, O. Farkas, D.K. Malick, A.D. Rabuck, K. Raghavachari, J.B. Foresman, J.V. Ortiz, Q. Cui, A.G. Baboul, S. Clifford, J. Cioslowski, B.B. Stefanov, G. Liu, A. Liashenko, P. Piskorz, I. Komaromi, R.L. Martin, D.J.

Fox, T. Keith, M.A., Al-Laham, C.Y. Peng, A. Nanayakkara, M.Challacombe, P.M.W. Gill, B. Johnson, W.Chen, M.W. Wong, C. Gonzalez, J.A. Pople, Gaussian03 D.01, Gaussian, Inc.: Pittsburgh, PA, (2003).

[10] H. B. Schlegel, *J. Comput. Chem.*, 3, 214 (1982).

[11] F. Jensen, *Introduction to Computational Chemistry*, Wiley, New York, (1999), p. 162.

[12] G. Rauhut, P. Pulay, *J. Phys. Chem.* 99, (1995), 3093.

[13] P. Sinha, S.E. Boesch, C. Gu, R.A. Wheeler, A.K. Wilson, *J. Phys. Chem. A*, 108, (2004), 9213.

[14] A.P. Scott, R. Radon, *J. Phys. Chem.* 100, (1996), 16502.

[15] T.M. Kolev, B.A. Stamboliyskaya, *Spectrochim. Acta Part A* 58, (2002), 3127.

[16] M. Pfeifer, F. Baier, T. Stey, D. Leusser, D. Stalke, B. Engels, D. Moigno, W. Kiefer, *J. Mol. Model.* 6, (2000), 299

[17] P.L. Fast, J. Corchado, M.L. Sanches, D.G. Truhlar, *J. Phys. Chem. A* 103 (1999) 3139.

[18] A.Frisch, A.B.Nelson, A.J.Holder, Gauss view, Inc.Pittsburgh PA, (2000).

[19] M.J.Dewar .H.N.Schmeising, *Tetrahedron* 5 (1959)166.

[20] J.P.Foster.F.Weinhold.*J.Am .Chem.Soc.*102(1980)7211

[21] Ocak I'skeleli, N. (2007). *Acta Cryst.* E63, 1997–1998

[22] Available from: <http://www.sigmaaldrich.com/spectra/rair/RAIR009454.PDF>.

[23] R.M. Badger, *J. Chem. Phys.* 2, (1934), 128.

[24] W.J. Gordy, *Chem. Phys.* 14 (5), (1946), 305.

[25] N.Sunderganesan, H.Saleem, S.MohanM.ramalingham, V.Sethuram, *acta crystallographica* vol-A, 62, (2005), page 740-751.

[26] C.Y.Panicker, H.T.Varghese, D.Philip.H.I. S.Nogueira, K.Kastkova, *Spectrochim.Acta* 67A (2007) 1313.

[27] J.A. Pople, H.B. Schlegel, R. Krishnan, D.J. Defrees, J.S. Binkley, M.J. Frisch, R.A. Whiteside, R.F. Hout, W.J. Hehre, *Int. J. Quant.Chem.* S15 (1981) 269.

[28] N.P.G.Roeges, *A Guide to complete interpretation of infrared spectra of organic structures*, Wiley, New York, 1974.

[29] J.A. Pople, H.B. Schlegel, R. Krishnan, D.J. Defrees, J.S. Binkley, M.J. Frisch, R.A. Whiteside, R.F. Hout, W.J. Hehre, *Int. J. Quant.Chem.* S15 (1981) 269.

[30] J.A. Pople, A.P. Scott, M.W. Wong, L. Radom, *Isr. J. Chem.* 33 (1993) 345.